Int. J. Heat Mass Transfer. Vol. 35, No. 7, pp. 1645–1657, 1992
Printed in Great Britain

0017–9310/92 $5.00 + 0.00

On natural convection in a single and two zone rectangular enclosure

T. G. KARAYIANNIS
Institute of Environmental Engineering, South Bank Polytechnic, 103 Borough Road, London SE1 0AA, U.K.

and

M. CIOFALO and G. BARBARO
Dipartimento di Ingegneria Nucleare, Università di Palermo, Viale delle Scienze, 90128 Palermo, Italy

(*Received* 29 *May* 1991 *and in final form* 15 *July* 1991)

Abstract—Convective heat transfer was investigated numerically for rectangular enclosures both undivided and divided in two zones by a vertical partition, and having opposite isothermal walls at different temperatures. The aspect ratio was varied from 0.1 to 16 and the Rayleigh number from $3.5 * 10^3$ to $3.5 * 10^7$ (non-partitioned enclosures) and from $1.0 * 10^5$ to $1.6 * 10^8$ (partitioned enclosures). The thickness and conductivity of the partition were varied. The end wall thermal boundary conditions were adiabatic or LTP (Linear Temperature Profile). The continuity, momentum and energy equations for a 2-D laminar steady flow were solved under the Boussinesq approximation by using a finite-difference method and the SIMPLEC pressure–velocity coupling algorithm. Grid-independent results indicate that the reduction in the Nusselt number caused by a thin central partition can be predicted within a few per cent (in the range investigated) by assuming the partition to be isothermal, i.e. infinitely conducting. The finite conductivity of the partition causes a temperature distribution along its length, resulting in an increase in Nu which depends on Rayleigh number, aspect ratio and end wall thermal boundary conditions.

1. INTRODUCTION

HEAT TRANSFER by natural convection in rectangular enclosures, such as the one shown in Fig. 1(a), is an area of considerable engineering interest. This is due to its many applications, such as in cavity walls, double-pane windows and solar collectors. Excellent reviews of the past experimental and numerical research work reporting on the flow patterns and heat transfer rates in rectangular enclosures are available and will not be discussed here [1–3].

Real thermal systems can deviate significantly from the simple rectangular cavity model of Fig. 1(a). For example, in building applications the model should include the association of two cavities communicating laterally through a doorway, window, corridor or over an incomplete dividing partition [4]. Natural convection in the air layer of a double-pane window is coupled with the internal natural convection in the room and external convection and could deviate from models such as the one shown in Fig. 1(a). Further, data obtained from the basic cavity model are not strictly applicable to the solar collector cavity where the internal convection is coupled with external convection at the glazing [5]. These and the possible insulating effect of partitions are some of the reasons which recently encouraged researchers to turn their attention to the study of convection in complex enclosures and, in particular, to enclosures with partial and complete partitions at the end walls.

The effect of partial partitions normal to the end walls on fluid flow and heat transfer in enclosures was investigated in refs. [6–14]. In the case of a completely partitioned enclosure the convection in the two resulting cavities is coupled, Fig. 1(b). Reports on this geometry are scarce and are only in general qualitative agreement, with disagreement in the actual numerical values which calls for further clarification. Anderson and Bejan [15] reported that N equidistant thin aluminium partitions in a water-filled enclosure having $AR = 1/3$ at $Ra = 10^9$–10^{11} reduced the overall heat transfer rate by a factor $(N+1)^{-0.61}$ (i.e. by a factor 0.65 for $N = 1$). Nishimura *et al.* [16] performed both an experimental and a numerical investigation. In their experiments the partitions were made of thin copper plates, the working fluid was water, the enclosure aspect ratio was 4 and 10 and the Rayleigh number ranged from 10^6 to 10^9; they found a heat transfer reduction factor of 0.42 for a single partition. From their numerical simulations ($AR = 4$, $Pr = 6$, $10^4 < Ra < 10^7$) the authors reported a reduction by a factor $(N+1)^{-1}$ (i.e. a factor 0.5 for $N = 1$).

2. MATHEMATICAL FORMULATION AND NUMERICAL METHODS

Figure 1 is a schematic of the basic, or non-partitioned, enclosure (identified with the subscript 'b') and of the partitioned enclosure (identified with the

NOMENCLATURE

AR	aspect ratio of the enclosure, H/W
b	thickness of the partition
g	acceleration due to gravity
H	height of the enclosure
k	thermal conductivity of the fluid
k_p	thermal conductivity of the partition (along y)
N_x, N_y	number of grid points along x and y
Nu_y	local Nusselt number, $qW/[(t_h - t_c)k]$
Nu	average Nusselt number, $(1/H)\int_{-H/2}^{H/2} Nu_y \, dy$
p	pressure
P	dimensionless pressure, $pW^2/(\rho\nu\alpha)$
Pr	Prandtl number, ν/α
q	local heat flux
r	dimensionless longitudinal thermal resistance of partition, see equation (8)
Ra	Rayleigh number, $g\beta(t_h - t_c)W^3/(\nu\alpha)$
t	temperature
T	dimensionless temperature, $(t - t_c)/(t_h - t_c)$
t_h	temperature of the hot wall
t_c	temperature of the cold wall
u	velocity along x (perpendicular to isothermal walls)
v	velocity along y (parallel to isothermal walls)
U, V	dimensionless velocities, $U = uW/\alpha$ and $V = vW/\alpha$
x, y	coordinates perpendicular and parallel to isothermal walls
X, Y	dimensionless coordinates, $X = x/W$ and $Y = y/W$
W	width of the enclosure.

Greek symbols

α	thermal diffusivity of the fluid
β	thermal expansion coefficient of the fluid
$\Delta x, \Delta y$	mesh sizes along x and y
ν	kinematic viscosity of the fluid
ρ	density of the fluid.

Subscripts

ad	indicates adiabatic conditions at the end walls
b	refers to the non-partitioned cavity
c	refers to the cold wall
h	refers to the hot wall
LTP	indicates Linear Temperature Profile conditions at the end walls
max	maximum
mon	monitoring point
p	refers to the partitioned cavity.

Superscripts

$'$	calculated for $r \to 0$ ('ideal' partition)
$''$	calculated for $r \to \infty$.

subscript 'p'). The enclosure has height H and width W. The dividing wall has a fixed thickness b. Following the Boussinesq approximation and the assumption of 2-D steady-state conditions the non-dimensional governing equations conform to the following form:

Continuity

$$\frac{\partial U}{\partial X} + \frac{\partial V}{\partial Y} = 0 \tag{1}$$

$$\frac{1}{Pr}\left[U\frac{\partial U}{\partial X} + V\frac{\partial U}{\partial Y}\right] = -\frac{\partial P}{\partial X} + \frac{\partial^2 U}{\partial X^2} + \frac{\partial^2 U}{\partial Y^2} \tag{2}$$

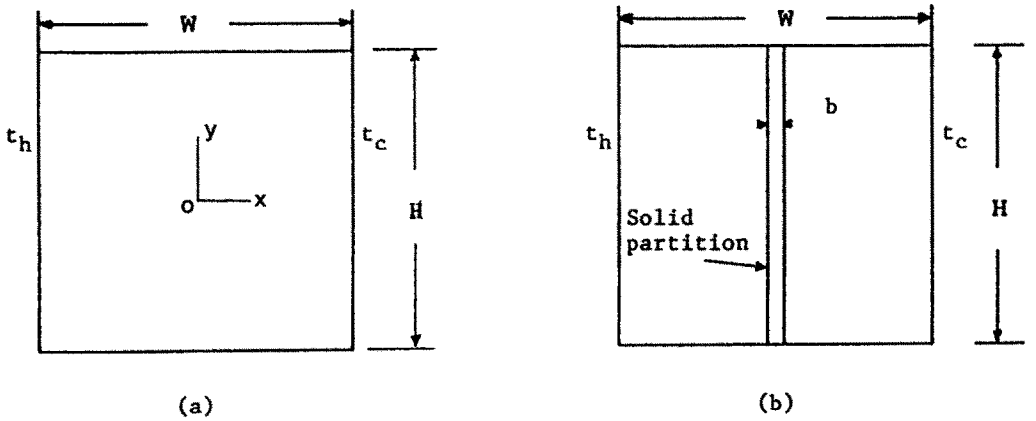

FIG. 1. Schematic of the basic (a) and partitioned (b) enclosure.

Momentum

$$\frac{1}{Pr}\left[U\frac{\partial V}{\partial X}+V\frac{\partial V}{\partial Y}\right]=-\frac{\partial P}{\partial Y}+\frac{\partial^2 V}{\partial X^2}+\frac{\partial^2 V}{\partial Y^2}+Ra\,T \tag{3}$$

Energy

$$U\frac{\partial T}{\partial X}+V\frac{\partial T}{\partial Y}=\frac{\partial^2 T}{\partial X^2}+\frac{\partial^2 T}{\partial Y^2} \tag{4}$$

and are coupled with the conduction equation in the solid partition. The non-dimensional variables X, Y, U, V, P and T are defined in the Nomenclature.

The flow boundary conditions are

$$U=V=0 \quad \text{on solid boundaries.} \tag{5}$$

The thermal boundary conditions at the isothermal walls are

$$T=1 \quad \text{at} \quad X=-1/2 \quad \text{(hot wall)} \tag{6a}$$

$$T=0 \quad \text{at} \quad X=1/2 \quad \text{(cold wall).} \tag{6b}$$

The thermal boundary conditions at the end walls can have a significant effect on local and mean heat transfer rates across the enclosure, especially at low aspect ratios [2, 12, 17]. Numerical investigations usually include adiabatic and LTP (Linear Temperature Profile) conditions, defined, respectively, by

$$\frac{\partial T}{\partial Y}=0 \tag{7}$$

$$T=\tfrac{1}{2}-X \tag{8}$$

with the former giving systematically higher heat transfer rates. In a recent comparison with experimental data [18] the present authors verified that heat transfer rates obtained experimentally and expected in real engineering systems (both for non-partitioned and partially partitioned cavities) should lie between these two boundary conditions and should be closer to the LTP. In this study both conditions are considered.

In the present investigation Ra was varied between $3.5*10^3$ and $3.5*10^7$ for the basic enclosures, and from $1.0*10^5$ to $1.6*10^8$ for the partitioned enclosures. The aspect ratio AR was varied between 0.1 and 16. Equations (1)–(4) were solved using the computer code Harwell-FLOW3D [19], which is based on a finite-difference, colocated-grid method. The SIMPLEC algorithm for pressure–velocity coupling was chosen [20].

In order to assess the effect of a partition on heat transfer rates from numerical simulations, it is crucial to obtain, for both the basic and the partitioned enclosure, fully converged and grid-independent results, based, as far as possible, on the same numerical methods. Thus, a preliminary analysis was conducted on the convergence behaviour of the solution with both the number of SIMPLEC iterations and the number and distributions of grid points. Examples of the results are shown below; they are all based on the central differencing scheme for the advective terms. Moderate underrelaxation factors (0.2–0.3) were used for the velocities and the temperatures so that the mass source residual (amount by which the continuity equation is *not* satisfied by the current solution) exhibited a smooth decreasing trend and eventually stabilized itself around 10^{-3}–10^{-4} times the overall mass flow associated with the main circulation cell.

Figure 2 illustrates the convergence behaviour of the solution with increasing iterations for a basic and a partitioned enclosure having $AR=1$, $Ra=10^6$ and LTP end walls. The vertical velocity v_{mon} at a monitoring location (around $X=Y=-1/4$) is reported as a function of the number of iterations as computed using two different grids having $30*30$ and $60*60$ nodes in the fluid, respectively, and selectively refined near solid walls. Convergence is slower for the finer grids and for the basic enclosure: there are still slight changes in the monitored quantity after 1500 iterations.

Figures 3(a) and (b) illustrate the grid dependence of the solution for basic and partitioned enclosures having $AR=1$ and 10, $Ra=10^6$ and LTP end walls. The maximum of the horizontal velocity, u_{max} (a) and the average Nusselt number (b) are reported against the number N_y of grid points along the vertical direction. The number of grid points in the horizontal direction is kept equal to N_y ($AR=1$) or $N_y/3$ ($AR=10$). The solution becomes grid independent at $N_y \geqslant 40$ for $AR=1$ and at $N_y \geqslant 90$ for $AR=10$. The average Nusselt number appears to be less sensitive than the velocity peak and, more generally, than the flow field.

On the basis of the above and similar results, the following computational grids were chosen for the final simulations for different values of the aspect ratio.

AR	0.1	0.2	0.5	1	2	3	5	10	16
N_x	90	80	70	60	50	56	40	50	30
N_y	30	40	50	60	70	74	80	90	120

The grids were selectively refined near solid walls following a linear stretching law with $\Delta x_{min}/\Delta x_{max} = \Delta y_{min}/\Delta y_{max} = 0.2$. Additional control volumes were used in the central partition if required.

The central differencing scheme (CDS) was used whenever possible for the advective terms in order to minimize numerical diffusion errors. For non-partitioned enclosures, up to $Ra=3.5*10^5$, results obtained by using CDS and hybrid-upwind differencing (HDS) differed negligibly both in Nu and in the peak velocities. For $AR>2$ and $Ra>10^6$ the CDS solution exhibited spurious oscillations and convergence was achieved only by using very small underrelaxation factors on U, V and T, while the difference in Nu between CDS and HDS results increased to about 1% (in the worst case, i.e. $AR=10$, LTP end

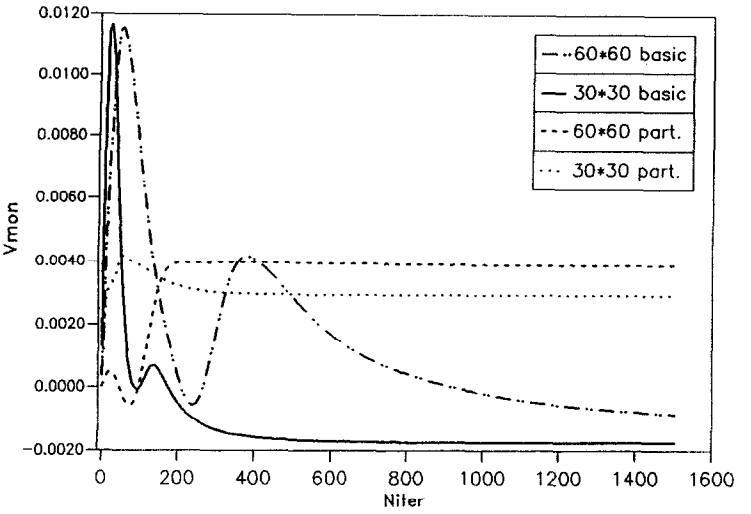

FIG. 2. Vertical velocity at a monitoring point as a function of the number of SIMPLEC iterations for $Ra = 10^6$, $AR = 1$, LTP end walls, basic or partitioned enclosure and two different grids.

walls). All results presented here for the basic enclosure are based on HDS at the highest Rayleigh numbers (10^7 and above) and on CDS otherwise. For the parametrical comparison study on the partitioned enclosure, HDS was mostly used. Computation times ranged from about 10 to about 30 min on an IBM 3090-200J, depending on Rayleigh number, aspect ratio, boundary conditions and partitioned/non-partitioned enclosure.

It should be observed that, for the basic enclosure, at high aspect ratios multicellular flow was predicted by using CDS, in agreement with experimental results and published high accuracy predictive studies [21, 22], but not by using HDS. Nevertheless, the corresponding average Nusselt number varied very little between the two cases, making the use of hybrid differencing quite acceptable for heat transfer predictions. The reason for this lies in that the details of the flow in the core region of the cavity have little influence on the near wall region, where most of the temperature variations occur. Incidentally, this is also the rationale for the use of two-dimensional, steady-state, laminar solutions even in cases where unsteadiness and three-dimensionality are known to occur in real enclosures.

3. PRELIMINARY ANALYSIS

3.1. *Results for the basic enclosure*

In the basic enclosure the Nusselt number is expected to be a function of the aspect ratio and the Rayleigh number, i.e.

$$Nu_b = f(AR, Ra). \tag{9}$$

At sufficiently high aspect ratio and Rayleigh number, it can be expressed with reasonable accuracy in the following way:

$$Nu_b = CAR^n\, Ra^m \tag{10}$$

where C, n and m are constants which can be determined from the correlation of experimental or numerical results.

Figures 4(a) and (b) show the average Nusselt number vs the Rayleigh number for adiabatic and LTP end walls and for $AR = 0.2$–10. An alternative way of presenting the results is to plot the average Nusselt number as a function of the aspect ratio for different values of Ra. This is shown in Fig. 5 for adiabatic (a) and LTP (b) end walls, respectively.

Comparison of numerical predictions with literature results, from both numerical and experimental work, is very good (see ref. [13]). Correlation equations for the present results are

$$AR = 1 \begin{cases} Nu = 0.155\, Ra^{0.29} \\ \quad \text{(adiabatic end walls)} & \text{(11a)} \\ Nu = 0.120\, Ra^{0.29} \\ \quad \text{(LTP end walls)} & \text{(11b)} \end{cases}$$

and

$$AR = 2\text{–}10 \begin{cases} Nu = 0.247\, AR^{-0.20}\, Ra^{0.26} \\ \quad \text{(adiabatic end walls)} & \text{(12a)} \\ Nu = 0.199\, AR^{-0.13}\, Ra^{0.26} \\ \quad \text{(LTP end walls).} & \text{(12b)} \end{cases}$$

The above correlations fit the results within $\pm 5\%$ of the range $Ra = 3.5 * 10^3$–$3.5 * 10^7$. One immediate observation from equations (12) is that

$$Nu_{\text{adiab}}/Nu_{\text{LTP}} \simeq 1.24\, AR^{-0.07} \tag{13}$$

which shows that the difference between the two values of Nu decreases with increasing AR, see also ref. [18], and is independent of Ra. If $AR = 1$, Nu is 24% higher for adiabatic than for LTP end walls.

As is obvious from Figs. 4 and 5, no simple power-

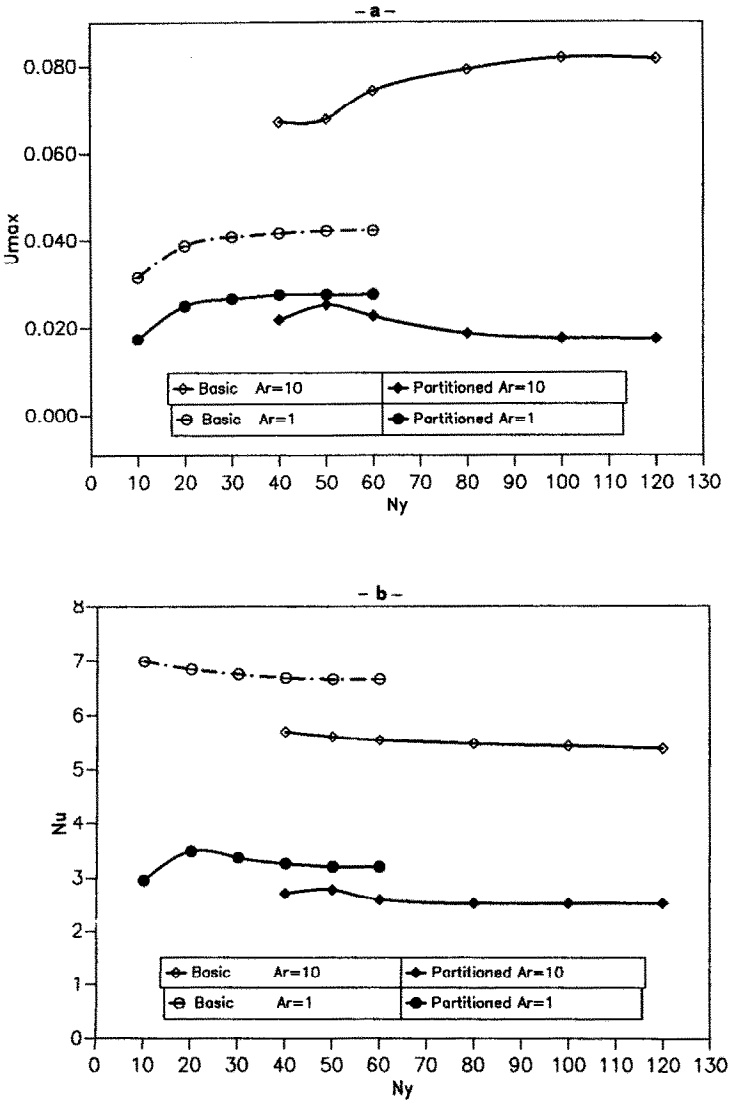

FIG. 3. Dependence of the results on the number of grid points along the vertical direction N_y, for $Ra = 10^6$, $AR = 1$ or 10 and basic or partitioned enclosures, (a) peak of horizontal velocity, (b) average Nusselt number.

law correlation is applicable to the results for very low aspect ratios ($AR < 1$) or Rayleigh numbers. It is convenient for the discussion that follows to represent Nu in graphical form by drawing the constant-Nu lines in the plane of the two independent parameters AR, Ra (both in log scales). The result is shown in Fig. 6 for adiabatic (a) and LTP (b) end walls, respectively. These graphs were drawn by interpolating predictive results relative to several hundred test cases.

3.2. *The expected effect of a partition on heat transfer*

3.2.1. *'Ideal' partition.* If an ideal, infinitely thin and perfectly conducting partition, isothermal at $T = 1/2$, centrally divides the enclosure then

$$AR_p = 2 * AR \tag{14a}$$

$$Ra_p = Ra/16 \tag{14b}$$

for each of the two separate cavities thus obtained. Hence

$$Nu_p = f(2 * AR, Ra/16). \tag{15}$$

This 'ideal' value, which is also the overall Nusselt number for the partitioned enclosure, will be indicated as Nu'_p in the following. If equation (10) can be used with constant n, m throughout the range AR–$2 * AR$, $Ra/16$–Ra then

$$Nu'_p/Nu_b = 2^{-(4m-n)}. \tag{16}$$

In particular, it follows from equations (12) that under these assumptions

$$Nu'_p/Nu_b = 2^{-1.24} = 0.423 \text{ (adiabatic end walls)} \tag{17a}$$

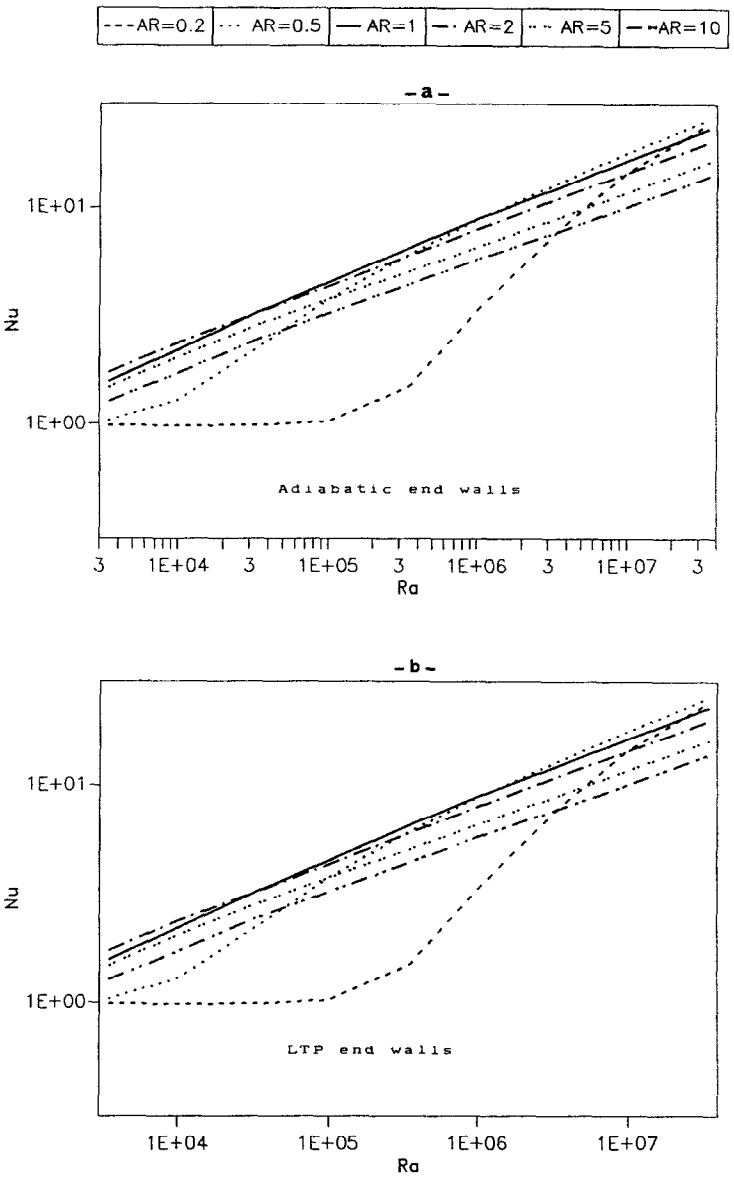

FIG. 4. Basic enclosure: average Nusselt number as a function of Ra for $AR = 0.2$–10 and adiabatic or LTP end walls.

$$Nu'_p/Nu_b = 2^{-1.17} = 0.444 \text{ (LTP end walls)}. \quad (17b)$$

For very high aspect ratios, the dependence of Nu on AR becomes negligible (i.e. $n \to 0$) and the reduction factor caused by the partition on Nu approaches 0.5.

More generally, the charts of Fig. 6 can be used. In order to find the effect of an 'ideal' partition on Nu one simply has to draw a segment corresponding (on log paper) to a 2-fold increase in AR and to a 16-fold decrease in Ra.

Point A in Fig. 6(b) is representative of the conditions investigated by Nishimura *et al.* [16], i.e. $AR = 5$, $Ra = 10^7$. The Nusselt number is about 11 for the basic enclosure. The construction described above leads to point A′ as representative of the corresponding 'ideal' partitioned enclosure; the associated Nusselt number is about 5, with a reduction factor of 0.44 in good agreement with the experimental result of ref. [16] (0.42). The same result can be obtained by using equation (17b).

On the other hand, point B in the same graph corresponds to $AR = 1/3$, $Ra = 3.5 * 10^7$ and is roughly representative of the experimental conditions investigated by Anderson and Bejan [15] (the authors performed their measurements for $Ra = 10^9$–10^{11}, which unfortunately is outside the range investigated here; however, the isopleths of Nu appear to be roughly parallel in the region around point B so that results

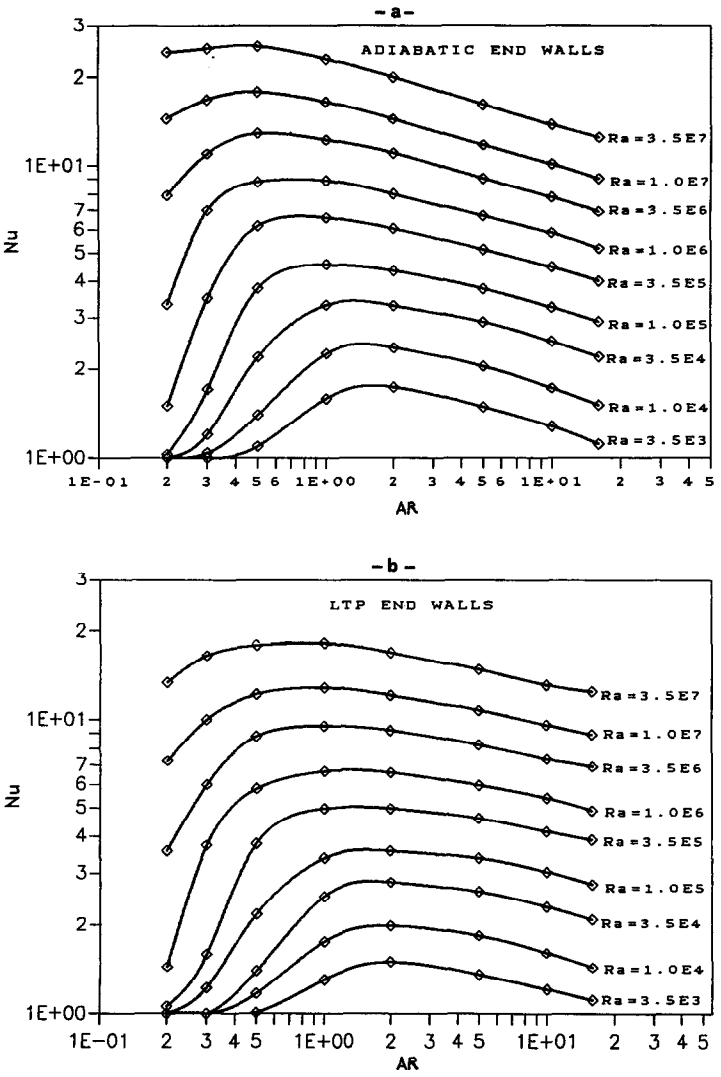

FIG. 5. Basic enclosure: average Nusselt number as a function of AR for $Ra = 3.5 * 10^3$–$3.5 * 10^7$ and adiabatic or LTP end walls.

can be extrapolated with little error). Proceeding as before, one finds a reduction in Nu from ~ 16 (point B) to ~ 9 (point B'), i.e. a reduction factor of about 0.56 in acceptable agreement with the experimental result of 0.65.

It should be observed that both the above experiments were performed in water ($Pr = 5$–6) while the present simulations are for air ($Pr = 0.72$); however, it is known that the Prandtl number has only a marginal influence on Nu [2]. LTP rather than adiabatic conditions at the end walls were used, as they are more appropriate to simulate the conditions of real laboratory experiments. Of course, due to the differences in Ra, Pr, thermal boundary conditions, etc. exact quantitative agreement with the results of refs. [15, 16] cannot be expected; nevertheless, the above discussion shows that the main differences in experimental results, concerning the effectiveness of partitions in reducing heat transfer rates in enclosures, can be explained even on the basis of the 'ideal' partition model. In particular, it should be observed that the reduction factor in Nu caused by a central partition may be much larger than 0.5 (i.e. the effectiveness of the partition may be very little) at very small aspect ratios (left region of the graphs in Fig. 6).

A similar technique may be used to assess the effect of multiple partitions; for example, two equidistant 'ideal' partitions cause a 3-fold increase in AR and a reduction in Ra by $(1/3)^4 = 1/81$. This results in a reduction factor of $3^{-1.17} = 0.276$ for LTP boundary conditions. This compares very well with the experimental results of Nishimura *et al.* [16] (Fig. 3).

3.2.2. *Real partition.* In the case of a real partition, having a finite thickness b and conductivity k_p, a departure from the 'ideal' behaviour occurs due to three distinct effects.

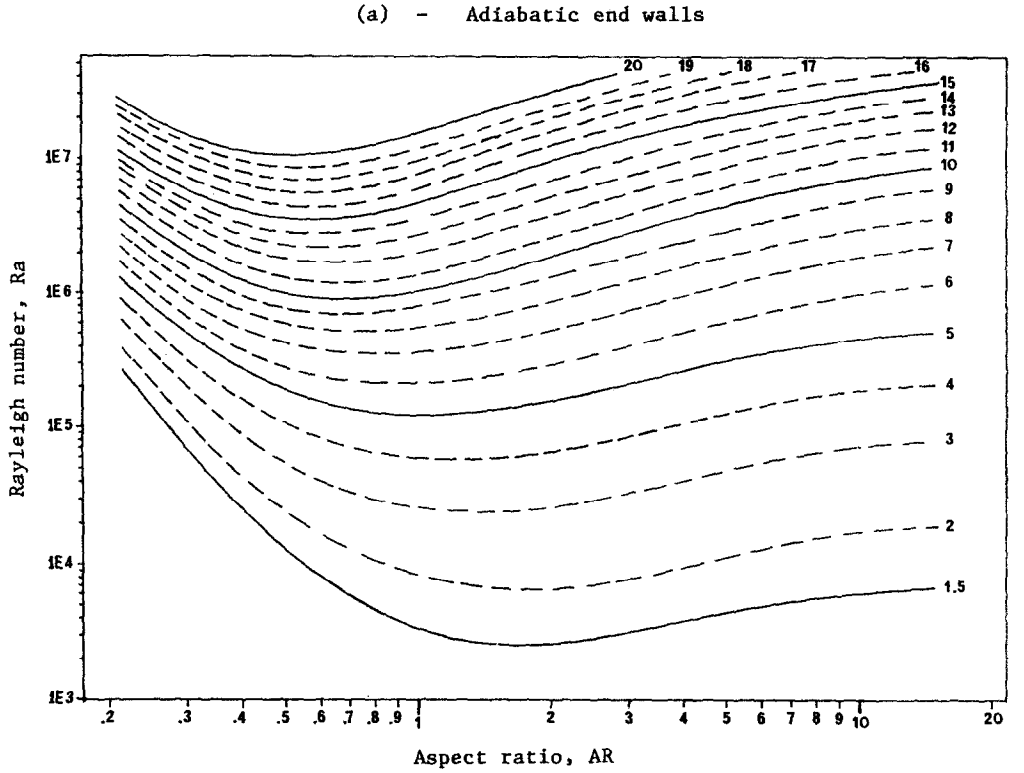

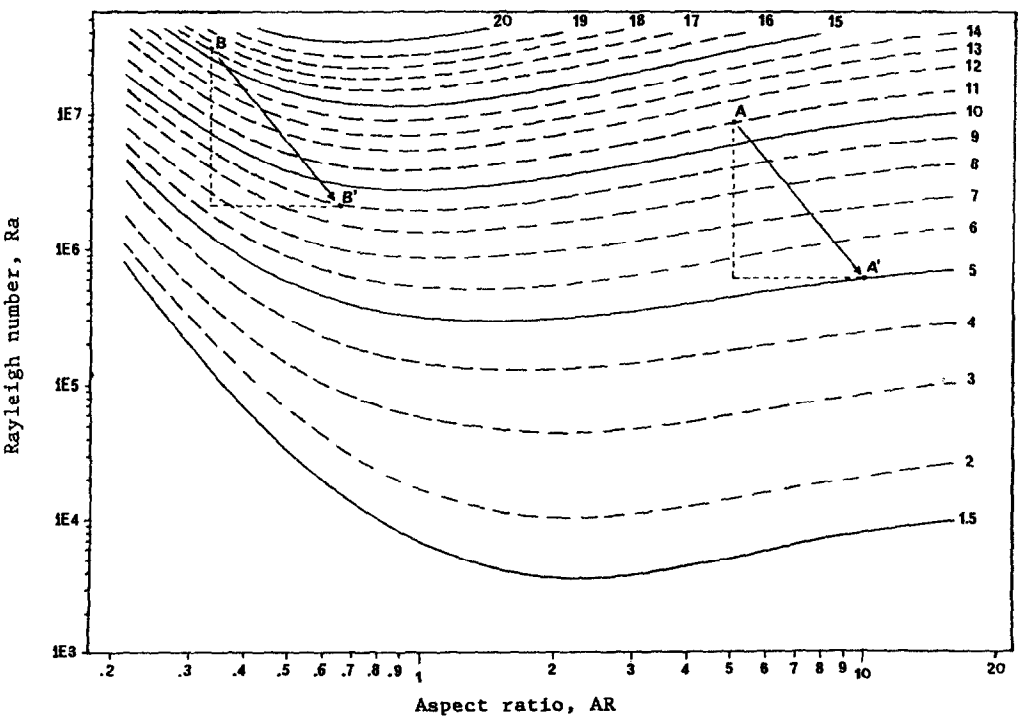

FIG. 6. Basic cavity: isopleths of *Nu* in the plane *AR–Ra* for adiabatic (a) and LTP (b) end walls. In (b) the method for predicting the effect of an 'ideal' partition is sketched.

(1) Geometrical effect—the partition reduces the width of each of the resulting separate cavities from $W/2$ to $(W-b)/2$, thus modifying the geometry of the problem. The 'partial' Rayleigh number of each separate cavity decreases, while the 'partial' aspect ratio increases, with respect to the 'ideal' case.

A simple, though cumbersome, analysis shows that, provided equation (10) holds and $b \ll W$, the overall Nusselt number changes by a factor $Nu_p/Nu'_p = 1 + (1-3m+n)b/W$ with respect to the 'ideal' case. For example, for LTP end walls and $AR > 1$ ('partial' aspect ratio > 2), equation (12b) is applicable yielding $Nu_p/Nu'_p = 1+0.09b/W$. Thus, the variation of Nu_p relative to Nu'_p caused by the finite thickness of the partition is positive and is less than 1% provided $b/W < 1/10$.

Only for 'partial' aspect ratios less than 1 (i.e. for $AR < 0.5$) the Nusselt number may increase markedly with the 'partial' aspect ratio, i.e. $n \cong 1$, which results in a relative variation of the overall Nusselt number Nu_p positive and of the same order of b/W.

(2) Thermal resistance effect—the partition adds its conductive thermal resistance along x, b/k_p, to the convective resistance of the fluid layers along the same direction, $W/(k\,Nu'_p)$, thus reducing the overall Nusselt number. A detailed analysis similar to that above shows that, provided $Nu'_p(b/W)(k/k_p) \ll 1$, the associated factor Nu_p/Nu'_p is $1-(1+m)Nu'_p(b/W)(k/k_p)$. Thus, this effect is always negligible for thin partitions ($b \ll W$) in air-filled enclosures ($k_p \gg k$). The variation of Nu_p is, of course, negative, i.e. opposite to that of the geometry change.

(3) Thermal coupling effect—the finite conductivity of the partition causes a complex temperature profile to be established along it, thus modifying the thermal boundary conditions of the two separate enclosures with respect to the 'ideal', isothermal-wall case. This effect becomes more important as the thickness of the central partitions decreases and the other two effects become negligible, therefore it is expected to be the most significant in air-filled enclosures with relatively thin partitions. The extent of the Nusselt number variation depends on the thermal conductance of the partition along the vertical direction, i.e. on the product $b*k_p$, rather than on these two parameters separately.

In order to single out the thermal coupling effect, several test cases were run by assuming a small partition thickness ($b/W = 1/40$), resolving the partition by four grid points, and setting its thermal conductivity along x to a very high (practically infinite) value. This assured effects (1) and (2) to be negligible, thus allowing the study of the major effect (3) without the disturbing influence of the other two. The conductivity k_p along y, and thus the partition's thermal resistance $1/(bk_p)$, were varied in a broad range between practically infinitely conducting (isothermal partition) and practically non-conducting (partition's vertical temperature profile completely imposed by the fluid). The capability of the Harwell-FLOW3D code to deal with anisotropic conduction in solids [19] was exploited to this purpose. Several aspect ratios and Rayleigh numbers, and adiabatic/LTP end walls, were tested. Results are summarized and discussed in the next section.

4. RESULTS AND DISCUSSION

Figure 7 compares predicted vertical profiles of Nu_y along the hot and cold walls, and partition temperature profiles, for the extreme cases $k_p \to \infty$ and $k_p \to 0$ and for adiabatic or LTP end walls, in a partitioned cavity having $AR = 5$ and $Ra = 10^7$. The corresponding average Nusselt numbers are also reported. The results shown are easily interpreted on the basis of the following considerations.

In an enclosure having a central partition, hot fluid from the hot wall impinges on the upper half of the partition while cold fluid from the cold wall impinges on the bottom half. Thus, the partition tends to be hotter at the top than at the bottom. When its longitudinal thermal resistance is small enough, heat will flow from the top to the bottom of the partition and an almost isothermal temperature profile will be established along it. On the other hand, when the longitudinal thermal resistance of the partition is large, compared with the effective thermal resistance of the fluid layers, a non-uniform temperature profile will be maintained along the partition. This results in increased heat transfer rates, as the temperature difference between hot wall and partition increases in the bottom half of the cavity, where the local hot-wall Nusselt number is large, and decreases in the top half, where it is small (the opposite occurs between the partition and cold wall). Also, the effect will be larger for a cavity having adiabatic rather than LTP end walls, as in the latter case the boundary conditions force the (dimensionless) temperature of the partition to be 1/2 both at the top and at the bottom ends, thus greatly limiting the temperature excursion along it.

The function describing the increase in Nu_p, as k_p decreases from infinity to zero, should possess a 'universal' nature, provided that the appropriate parameter is used as the independent variable. By carefully analysing the present results, it was concluded that the most appropriate parameter is the ratio of the thermal resistance per unit length of the partition along y, $1/(bk_p)$, to the equivalent thermal resistance per unit length of the fluid layers along x in the basic enclosure, $1/(Hk\,Nu_b)$

$$r = \frac{1/(bk_p)}{1/(Hk\,Nu_b)} = \frac{Nu_b\,AR}{(k_p/k)(b/W)}. \tag{18}$$

Figure 8 shows the average Nusselt number in the partitioned enclosure, normalized to its 'ideal' value Nu'_p (15), as a function of r for different combinations of aspect ratios and Rayleigh numbers. Adiabatic end walls are assumed; similar curves, but with lower departures from the 'ideal' behaviour, are obtained

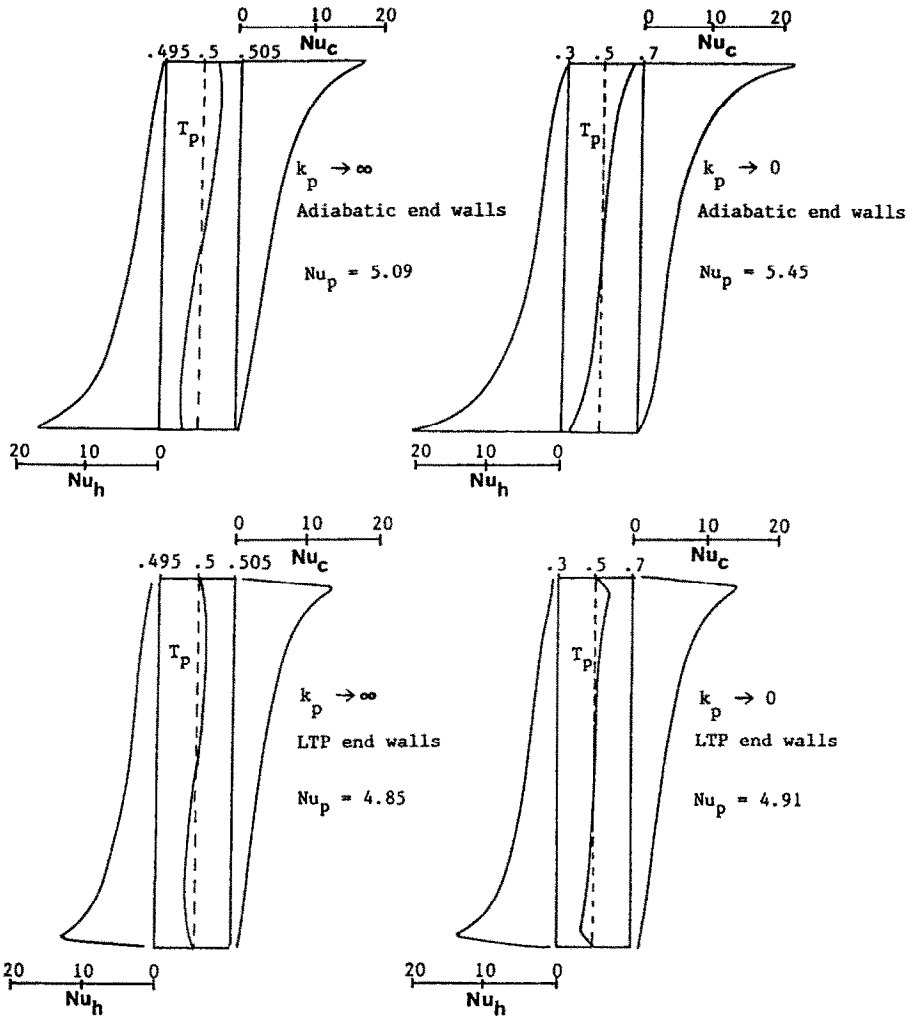

FIG. 7. Effect of the finite longitudinal thermal resistance of the partition on profiles of Nu_y and of the partition temperature for adiabatic and LTP end walls ($AR = 5$, $Ra = 10^7$).

for LTP end walls. In all cases, Nu_p is practically coincident with Nu'_p for $r < 10^{-3}$ and reaches a maximum Nu''_p for $r > 10^3$. It is evident that $(Nu_p - Nu'_p)/(Nu''_p - Nu'_p)$ is a fairly universal function of r only. Its behaviour is (rather crudely) described by

$$(Nu_p - Nu'_p)/(Nu''_p - Nu'_p) = 1/(1 + r^{-0.87}). \quad (19)$$

It should be observed that the value of r depends not only on the relative thickness (b/W) and conductivity (k_p/k) of the partition, but also on AR and Nu_h (hence on Ra).

For example, for a double-glazed window having $H = 60$ cm, $W = 6$ cm, $t_h - t_c = 20°C$, one has $AR = 10$, $Ra = 4 * 10^5$ and, from equations (12), $Nu_h = 4.2$–4.5. A central glass partition 0.2 cm thick $(k_p/k = 30, b/W = 1/30)$ has an r-value of ~ 35. This is far from the 'ideal' case $r \to 0$ (perfectly conducting, or isothermal, partition), being rather closer to the case $r \to \infty$, see Fig. 8. In fact, from equation (19) one has

$$(Nu_p - Nu'_p)/(Nu''_p - Nu'_p) = 0.96.$$

The maximum relative increase in Nu_p, $\Delta Nu = (Nu''_p - Nu'_p)/Nu'_p$ (corresponding to a partition having infinite thermal resistance along y, i.e. to a thin foil) is shown in Fig. 9 as a function of Ra for $AR = 5$ and adiabatic or LTP end walls. In the former case, ΔNu increases monotonically with Ra. For LTP end walls, ΔNu has a flat maximum about $Ra = 10^6$ and is always much lower (2–5 times) than for adiabatic end walls.

The dependence of ΔNu on Ra and AR was investigated in more detail for the adiabatic case only. Figure 10 shows ΔNu as a function of AR for $Ra = 1.6 * 10^5$–$1.6 * 10^8$. At low Rayleigh numbers, ΔNu increases monotonically with AR up to $AR = 10$; at higher Ra, a maximum appears which is located around $AR = 2$–3 and becomes more pronounced with increasing Ra.

In the range investigated, ΔNu never exceeds $\sim 12\%$

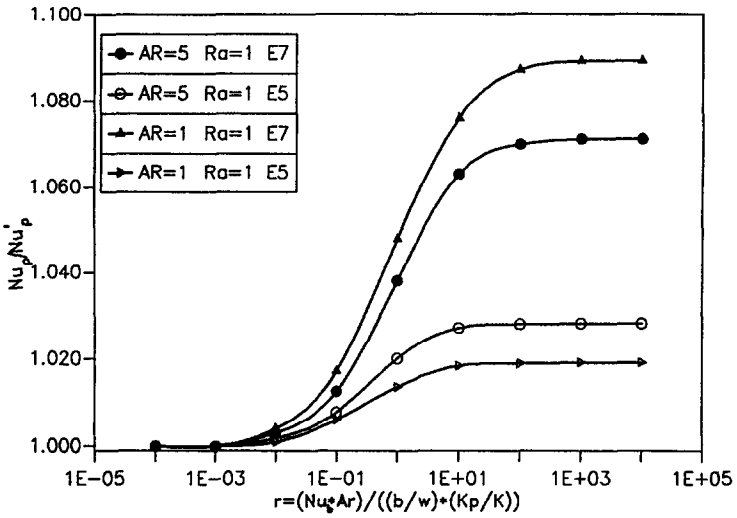

FIG. 8. Average Nusselt number as a function of the parameter r for different aspect ratios and Rayleigh numbers (adiabatic end walls). Values are normalized to those for $r \to 0$.

(adiabatic end walls) or $\sim 3\%$ (LTP end walls). For the double-glazed window example considerd above, it follows from Fig. 10 that, even in the case of adiabatic end walls, $\Delta Nu \cong 3\%$. Thus, the 'ideal' value Nu'_p, obtained by using the charts in Fig. 6 or, when possible, correlations (12) or similar, can be used as a fair approximation for Nu_p in practical engineering calculations, especially those concerning air-filled enclosures.

In the experiments of Nishimura *et al.* [16] the ratio r is approximately 7.5 which for LTP boundary conditions gives only a marginal ($<1\%$) deviation from the ideal case.

5. CONCLUSIONS

The effect of a central partition on heat transfer rates in a rectangular vertical enclosure of height H and width W, having opposite isothermal walls at temperatures t_h, t_c was investigated numerically.

If the partition can be assumed to be 'ideal', i.e. infinitely thin and isothermal at $(t_h+t_c)/2$, the resulting reduction in heat transfer rates from Nu_b to Nu_p can be simply computed from accurate results $Nu = f(AR, Ra)$ relative to vertical rectangular enclosures; such results, based on highly accurate and grid-independent numerical simulations, were pre-

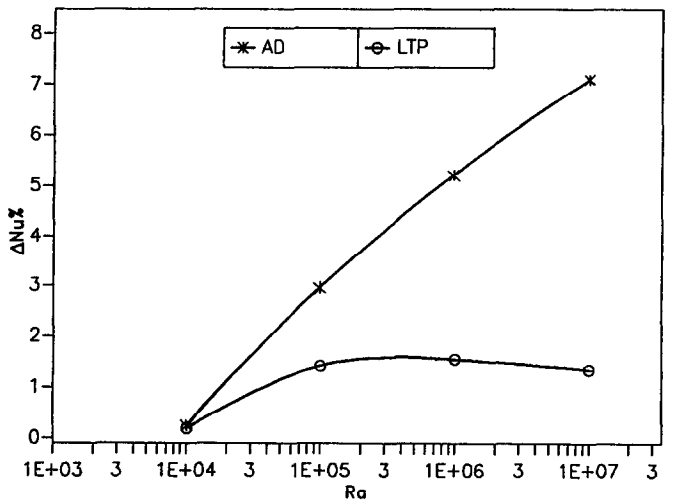

FIG. 9. Maximum relative increase in Nu_p due to the finite thermal resistance of the central partition as a function of Ra for $AR = 5$ and adiabatic or LTP end walls.

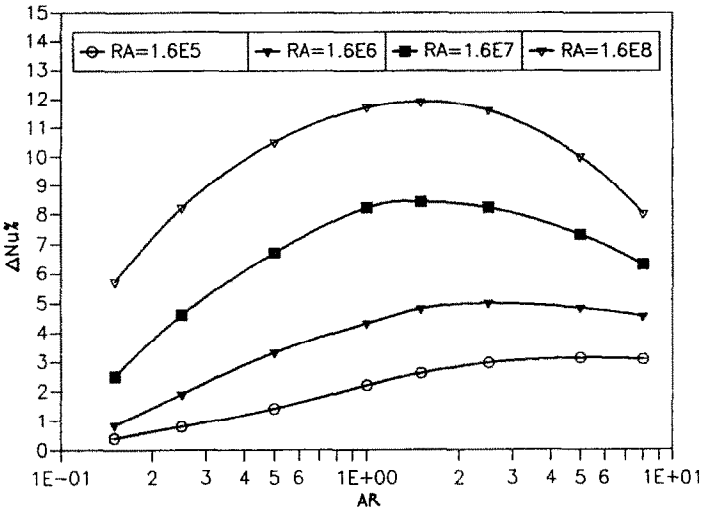

FIG. 10. Maximum relative increase in Nu_p due to the finite thermal resistance of the central partition as a function of AR for various Ra (adiabatic end walls only).

sented in graphical form for $AR = 0.1$–16 and $Ra = 3.5 * 10^3$–$3.5 * 10^7$, and in correlation form for $AR > 1$ and the same range of Ra.

For a real partition, having finite thickness b and conductivity k_p, a departure from this 'ideal' behaviour occurs. If the cavity is air-filled and the partition is relatively thin, the main reason for this departure is the thermal coupling of the two separate enclosures across the partition. This effect was isolated and numerically investigated for a wide range of AR, Ra and partition conductivities. A dimensionless parameter r, expressing the ratio of the thermal resistance of the partition along y to the effective resistance of the fluid layers along x, was introduced and was found to characterize well the amount of departure from the 'ideal' (perfectly isothermal partition) behaviour. For any given AR and Ra, for $r < 10^{-3}$ Nu_p is close to its 'ideal' value Nu_p', while for $r > 10^3$ it approaches a maximum Nu_p''. The relative increase in Nu_p was found to depend on AR and Ra and, much more sensitively, on the end wall boundary conditions, being far larger for adiabatic than for LTP ones. In the range investigated, it never exceeded the value of $\sim 12\%$ (adiabatic) or $\sim 3\%$ (LTP). Thus, the use of the 'ideal' value of Nu_p is quite acceptable in practical engineering applications concerning air-filled enclosures.

REFERENCES

1. I. Catton, Natural convection in enclosures, *Proc. 6th Int. Heat Transfer Conf.*, Toronto, pp. 13–30 (1978).
2. W. M. M. Schinkel, Natural convection in inclined air-filled enclosures, Dutch Efficiency Bureau, Pijnacker (1980).
3. K. T. Yang, Transitions and bifurcations in laminar buoyant flows in confined enclosures, *ASME J. Heat Transfer* **110**, 1191–1204 (1988).
4. A. Bejan, *Convection Heat Transfer*. Wiley, New York (1984).
5. T. G. Karayiannis and J. D. Tarasuk, Natural convection in an inclined rectangular cavity with different thermal boundary conditions at the top plate, *ASME J. Heat Transfer* **110**, 350–357 (1988).
6. M. W. Nansteel and R. Greif, Natural convection in undivided and partially divided rectangular enclosures, *ASME J. Heat Transfer* **103**, 623–629 (1981).
7. M. W. Nansteel and R. Greif, Natural convection heat transfer in complex enclosures at large Prandtl number, *ASME J. Heat Transfer* **105**, 912–915 (1983).
8. K. H. Winters, Laminar natural convection in a partially divided rectangular cavity at high Rayleigh number, *Int. J. Numer. Methods Fluids* **8**, 247–281 (1988).
9. S. M. Bajorek and J. R. Lloyd, Experimental investigation of natural convection in partitioned enclosures, *ASME J. Heat Transfer* **104**, 527–531 (1982).
10. L. C. Chang, J. R. Lloyd and K. T. Yang, A finite difference study of natural convection in complex enclosures, *Proc. 7th Int. Heat Transfer Conf.*, Munich, Vol. 2, pp. 183–188 (1982).
11. S. M. Bilsky, J. R. Lloyd and K. T. Yang, An experimental investigation of the laminar natural convection velocity field in square and partitioned enclosures, *Proc. 8th Int. Heat Transfer Conf.*, San Francisco, Vol. 4, pp. 1513–1518 (1986).
12. M. Ciofalo and T. G. Karayiannis, Natural convection in a rectangular partitioned cavity, *Proc. 7th Natn. Conf. UIT (Unione Italiana di Termofluidodinamica)*, Florence, Italy, pp. 31–55 (1989).
13. M. Ciofalo and T. G. Karayiannis, Convective heat transfer in a vertical rectangular cavity with partitions at the end walls, *Proc. 9th Int. Heat Transfer Conf.*, Jerusalem, Vol. 5, pp. 297–303 (1990).
14. S. D. Probert and J. Ward, Improvements in the thermal resistance of vertical, air-filled, enclosed cavities, *Proc. 5th Int. Heat Transfer Conf.*, Japan, Vol. 3, pp. 124–128 (1974).
15. R. Anderson and A. Bejan, Heat transfer through single and double vertical walls in natural convection—theory and experiment, *Int. J. Heat Mass Transfer* **24**, 1611–1620 (1981).
16. T. Nishimura, M. Shiraishi, F. Nagasawa and Y. Kawamura, Natural convection heat transfer in enclosures with multiple vertical partitions, *Int. J. Heat Mass Transfer* **31**, 1679–1686 (1988).
17. S. M. Elsherbiny, K. G. T. Holland and G. T. Raithby, Effect of the thermal boundary conditions on natural

convection in vertical and inclined air layers, *Proc. 20th ASME-A.I.Ch.E. Natn. Heat Transfer Conf.*, Wisconsin, HT Vol. 16, pp. 127–133 (1981).
18. M. Ciofalo and T. G. Karayiannis, Natural convection heat transfer in a partially- or completely-partitioned vertical rectangular enclosure, *Int. J. Heat Mass Transfer* **34**, 167–179 (1991).
19. A. D. Burns, I. P. Jones, J. R. Kightley and N. S. Wilkes, Harwell-FLOW3D, Release 2.1; User Manual, UKAEA Report AERE-R (Draft), August (1988).
20. J. P. Van Doormal and G. D. Raithby, Enhancements of the SIMPLE method for predicting incompressible fluid flows, *Numer. Heat Transfer* **7**, 147–163 (1984).
21. G. Lauriat and G. Desrayaud, Natural convection in air-filled cavities of high aspect ratios: discrepancies between experimental and theoretical results, *Int. J. Heat Mass Transfer* **34**, 167–179 (1991).
22. P. Le Quere, A note on multiple and unsteady solutions in two-dimensional convection in a tall cavity, *ASME J. Heat Transfer* **112**, 965–974 (1990).

SUR LA CONVECTION NATURELLE DANS UNE CAVITE RECTANGULAIRE A UNE OU DEUX ZONES

Résumé—Le transfert thermique convectif est étudié numériquement pour des cavités rectangulaires sans partition ou divisées en deux zones par une cloison verticale et ayant des parois opposées isothermes à différentes températures. Le rapport de forme varie de 0,1 à 16 et le nombre de Rayleigh de $3{,}5 \times 10^3$ à $3{,}5 \times 10^7$ (sans partition) et de $1{,}0 \times 10^5$ à $1{,}6 \times 10^8$ (avec partition). On fait varier l'épaisseur et la conductivité de la cloison. Les conditions aux limites thermiques aux parois terminales sont adiabatiques ou PTL (profil de température linéaire). Les équations de continuité, de momentum et d'énergie pour un écoulement 2-D laminaire permanent sont résolues dans l'approximation de Boussinesq en utilisant une méthode de différences finies et un algorithme de couplage pression–vitesse. Des résultats indépendants de la grille indiquent que la réduction du nombre de Nusselt causée par une cloison centrale mince peut être prédite à un faible pourcentage (dans le domaine étudié) en supposant la partition isotherme, c'est-à-dire infiniment conductrice. La conductivité finie de la cloison cause une distribution longitudinale de température avec un accroissement de *Nu* qui dépend du nombre de Rayleigh, du rapport de forme et des conditions aux limites thermiques sur les parois terminales.

NATÜRLICHE KONVEKTION IN EINEM IN EINE ODER ZWEI ZONEN UNTERTEILTEN HOHLRAUM

Zusammenfassung—Es wird der konvektive Wärmeübergang in einem rechteckigen Hohlraum numerisch untersucht, der entweder durch eine vertikale Wand in zwei Zonen unterteilt ist oder auch nicht. Der Hohlraum besitzt zwei gegenüberliegende isotherme Wände unterschiedlicher Temperatur. Das Seitenverhältnis wird zwischen 0,1 und 16 variiert, die Rayleigh-Zahl von $3{,}5 \times 10^3$ bis $3{,}5 \times 10^7$ (im nicht-unterteilten Hohlraum) bzw. von $1{,}0 \times 10^5$ bis $1{,}6 \times 10^8$ (im unterteilten Hohlraum). Die Dicke und Wärmeleitfähigkeit der unterteilenden Wand wird ebenfalls variiert. Die Endwand ist entweder adiabat, oder ihr wird ein lineares Temperaturprofil aufgeprägt. Die Gleichungen für Kontinuität, Impulstransport und Energie werden für eine zweidimensionale laminare stationäre Strömung gelöst, und zwar unter den Annahmen der Boussinesq-Approximation. Hierzu wird ein Finite-Differenzen-Verfahren und der SIMPLEC-Algorithmus für die Kopplung von Druck und Geschwindigkeit verwendet. Die gitterunabhängigen Ergebnisse zeigen, daß die Verringerung der Nusselt-Zahl durch eine dünne Unterteilung in der Mitte innerhalb einiger weniger Prozent vorhergesagt werden kann (für den untersuchten Bereich), wenn die Unterteilung als isotherm, d. h. unendlich gut leitend betrachtet wird. Für den Fall einer endlichen Leitfähigkeit ergibt sich eine Temperaturverteilung an der Trennwand, wodurch die Nusselt-Zahl zunimmt. Diese hängt von der Rayleigh-Zahl, vom Seitenverhältnis und von der thermischen Randbedingung an der Endwand ab.

ЕСТЕСТВЕННАЯ КОНВЕКЦИЯ В ОДНО- И ДВУХЗОННОЙ ПОЛОСТИ ПРЯМОУГОЛЬНОГО СЕЧЕНИЯ

Аннотация—Численно исследовался конвективный теплоперенос в прямоугольных полостях как неразделенных, так и разделенных на две зоны вертикальной перегородкой и имеющих различные температуры противоположных изотермических стенок. Отношение сторон варьировалось от 0,1 до 16, а число Рэлея от $3{,}5 \times 10^3$ до $3{,}5 \times 10^7$ (для неразделенных полостей) и от $1{,}0 \times 10^5$ до $1{,}6 \times 10^8$ (для разделенных полостей). Толщина и теплопроводность перегородки изменялись. Тепловые граничные условия на торцевых стенках были адиабатическими или соответствовали линейному температурному профилю. С использованием конечно-разностного метода и алгоритма SIMPLEC, связывающего двление со скоростью, решались уравнения неразрывности, а также сохранения количества движения и энергии для двумерного ламинарного стационарного течения в приближении Буссинеска. Результаты, не зависящие от выбора сетки, показывают, что уменьшение числа Нуссельта, вызванное тонкой центральной перегородкой, может быть определено с точностью до нескольких процентов (в исследуемом диапазоне) в предположении изотермичности перегородки, т.е. ее бесконечной теплопроводности. Конечная теплопроводность перегородки обусловливает распределение температур по ее длине, приводящее к увеличению значения *Nu*, которое зависит от числа Рэлея, отношения сторон и тепловых граничных условий на торцевых стенках.